Vol.67: e24220594, 2024
https://doi.org/10.1590/1678-4324-2024220594
ISSN 1678-4324 Online Edition

BABT
Brazilian Archives of Biology and Technology

Article - Engineering, Technology and Techniques

Effect of Load Size on Power Absorbed During Microwave Heating in a Cavity: Electromagnetic Modeling and Experimental Validation

Jhony Tiago Teleken[1*]
https://orcid.org/0000-0003-3642-8124

Bruno Augusto Mattar Carciofi[2]
https://orcid.org/0000-0002-9233-0984

[1]Universidade Federal do Maranhão, Departamento de Engenharia Química, São Luiz, MA, Brasil; [2]Universidade Federal de Santa Catarina, Departamento de Engenharia Química e Engenharia de Alimentos, Florianópolis, SC, Brasil.

Editor-in-Chief: Alexandre Rasi Aoki
Associate Editor: Alexandre Rasi Aoki

Received: 03-Aug-2022; Accepted: 13-May-2024.

*Correspondence: jtteleken@gmail.com (J.T.T.).

HIGHLIGHTS

- A theoretical model has been developed to evaluate the microwave heating in a domestic oven.
- The energy efficiency is function of the sample size.
- Small samples obtain better heating uniformity.

Abstract: The effect of material size on the amount and uniformity of power absorbed during microwave heating was evaluated by numerical and experimental methods. A three-dimensional (3D) mathematical model, based on the Maxwell's equations of electromagnetism, was solved using the Finite Element Method to predict the power dissipated in the sample. Experimental analysis was performed using a domestic oven and distilled water. Experimental and numerical results showed a good agreement to each other. However, a complex relationship exists between sample size and absorbed power. The modification of the resonance modes in the oven when the sample size is changed may explain it. Furthermore, heating uniformity decreases as the water load size increases because microwave power dissipation occurs mostly near the sample surface due to a lower intensity of resonances inside large samples.

Keywords: Numerical simulation; microwave heating pattern; load size.

INTRODUCTION

Microwave ovens are common kitchen appliances in many households. They have become popular mainly for their practical and rapid way of reheating food. Microwave heating also has been used in many food processing applications, like cooking [1], drying [2,3], thawing [4], pasteurization, and sterilization [5]. Electromagnetic radiation in the microwave frequency (915 MHz or 2450 MHz) heats the food by using two mechanisms: dipole rotation and ionic conduction, both caused by the oscillatory polarization of the electric field inside the material. This phenomenon promotes the food's volumetric heating, leading to a higher thermal efficiency and a shorter processing time than traditional heating methods [6].

The electromagnetic power converted into thermal energy in a microwave oven is affected by several factors that present complex interactions, including the design of the oven cavity [7,8], the microwave frequency [9], and food parameters, such as dielectric properties [10], shape [11,12], and size [13]. Such factors can modify the amount and uniformity of the energy dissipated in the food. The non-uniformed volumetric heating is the main concern for the use of microwave in industrial processes due to its impacts on food safety and quality [6].

The microwave power dissipation inside food is related to the local electric field as established by the Poynting's theorem. The electric field distribution is described by the Maxwell's equations of electromagnetism [14]. Mathematical models based on Maxwell's equations are commonly used for simulation analysis of heating processes in microwave ovens because their solutions characterize the exact microwave propagation dynamics [4,15–17]. Computer-aided studies based on Maxwell's equations are an effective tool for examining the causes of changes in microwave power dissipation and finding cause-effect relationships with process conditions. Such relationships can help developers of microwavable food products and microwave ovens, reducing costs and time during the design of process, equipment, and products.

With computer-aided engineering, process and product design based on prototypes can shift to a model-based approach that simulates a virtual representation of the product or process. This reduces the need for prototypes, minimizes trial-and-error experimentation, and reduces time to market and resource use [18]. For example, Chen and coauthors [19] used numerical simulation to evaluate the effect of a susceptor (a metalized film attached to paperboard) on heating frozen food in a package in microwave ovens. Similarly, Jung and coauthors [20] used numerical simulation to evaluate the effect of container (packaging) design on the temperature distribution inside the food during microwave heating. Regarding process design, Costa and coauthors [21] designed a hexagonal microwave dryer using numerical simulations, while Salvador and coauthors [15] evaluated the effect of the number of magnetrons on the electric field distribution inside the cavity.

In this context, the objective of this work was to evaluate the effect of material size (cylindrical shaped) and dimensions (radius vs. height) during heating in a microwave oven. A three-dimensional (3D) electromagnetic model based on Maxwell's equations was developed to quantify the power dissipated in the material, and the uniformity of heating was evaluated based on the coefficient of variation (COV) of the microwave power density. The validation was based on experimental data of power dissipated in water loads heated in a household microwave oven.

MATERIAL AND METHODS

Experimental procedure

The experimental analyses were performed using a household microwave oven with a cavity volume of 45 dm³, operating at 2450 MHz, and a rated power of 1000 W (Electrolux, MEX55, Brazil). Eight loads of distilled water (m_w = 2.0, 1.5, 1.0, 0.8, 0.5, 0.4, 0.25, and 0.15 kg) and griffin beakers of borosilicate glass (2.0, 1.0, 0.6, 0.25, and 0.15 dm³) were used. The geometric parameters of each sample are summarized in Table 1.

Table 1. Dimensions of beakers and water loads (water density, ρ_W = 1000 kg m^{-3} = 1 kg dm^{-3}).

	Beaker griffin			Water	
Beaker volume – Water volume	**Inner diameter (mm)**	**Wall thickness (mm)**	**Weight (kg)**	**Height (mm)**	**Surface area (cm²)**
2.00 dm³ - 2.00 dm³	126	2.0	0.444	161.95	867.15
2.00 dm³ - 1.50 dm³	126	2.0	0.444	121.75	707.94
1.00 dm³ - 1.00 dm³	101	2.0	0.272	126.05	545.84
1.00 dm³ - 0.80 dm³	101	2.0	0.272	101.00	465.81
0.60 dm³ - 0.50 dm³	86	2.0	0.184	86.95	341.41
0.60 dm³ - 0.40 dm³	86	2.0	0.184	69.70	294.36
0.25 dm³ - 0.25 dm³	66	2.0	0.100	73.40	217.50
0.15 dm³ - 0.15 dm³	56	2.0	0.090	61.20	154.40

The absorbed power was determined thermodynamically based on the water temperature variation, according to previous works [22,23]. The empty beaker was weighed (m_b), filled with water at 25±1 °C, weighed again (m_w), and inserted into the cavity over the polypropylene table fixed at the oven's bottom.

Polypropylene was selected because it is a nontoxic material with a very low loss tangent (tan δ = 0.0003–0.0004); in other words, the microwave energy dissipated in the table is negligible [24]. The size details of the experimental apparatus and the specific position of the water load inside the cavity are illustrated in Figure 1. The heating process was carried out until the water reached 35±2 °C to avoid energy losses by evaporation and substantial changes in the dielectric properties of water. The final temperature (T_f) was measured using a previously homogenized liquid and a mercury thermometer. The power (P_{exp}) was then calculated using Equation 1.

$$P_{exp} = \frac{c_{p,w} m_w (T_f - T_0) + c_{p,b} m_b (T_f - T_0)}{t} \quad (1)$$

where $c_{p,w}$ (4.18 kJ (kg°C)$^{-1}$ [25]) and $c_{p,b}$ (0.75 kJ (kg°C)$^{-1}$ [26]) are the specific heat of water and borosilicate glass, respectively, T_0 is the initial temperature, and t is the heating time that was specified in the oven control panel. Before the experiments to obtain P_{exp}, the t value was estimated experimentally from trial and error for each water load. The experimental tests for P_{exp} were repeated four times for each water load. The International Electrotechnical Commission's Stander suggests using water load to estimate power dissipation in microwave ovens (No – 60705: Household microwave ovens - Methods for measuring performance) [23].

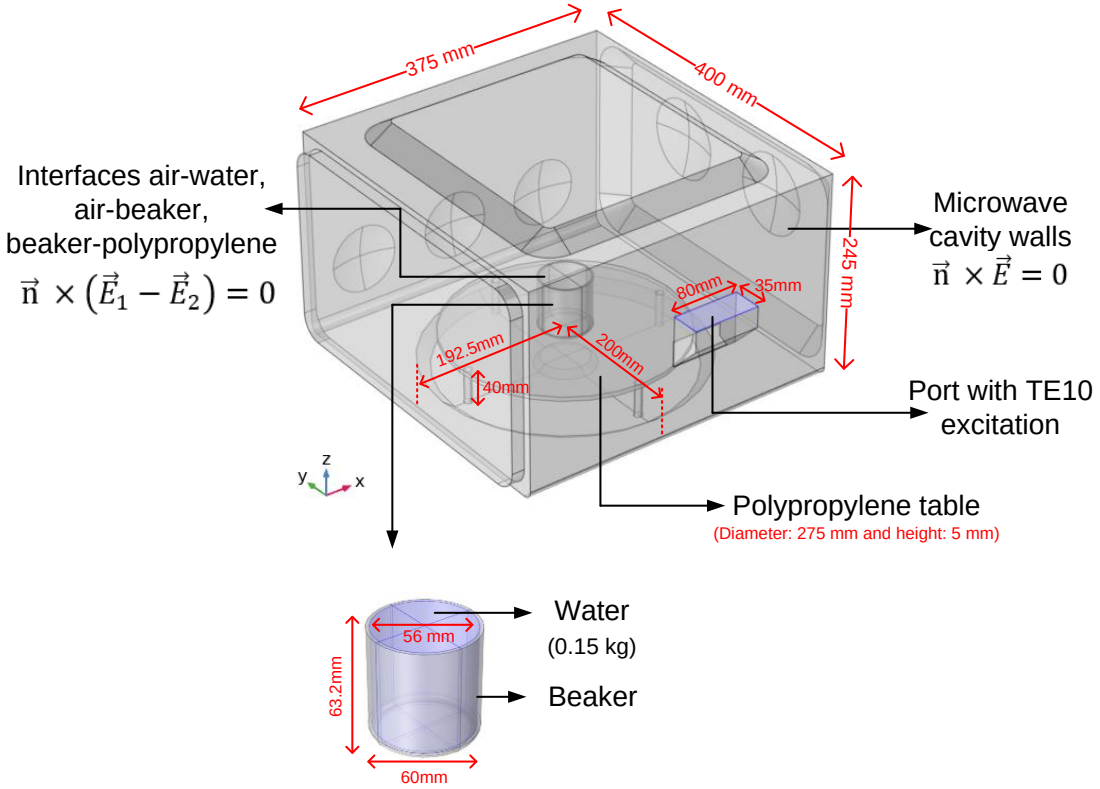

Figure 1. Three-dimensional (3D) computational domain model for a 0.15 kg water load.

Mathematical modeling

Figure 1 illustrates the computational domain of the electromagnetic model, which includes a detailed description of the cavity, waveguide, polypropylene table, beaker, and water load. The mathematical model assumed that (i) dielectric properties of materials are constant, (ii) energy loss from water to its surrounding is negligible, and (iii) the water remains at rest. The study focused on the effect of load size on microwave power absorption. Therefore, the study did not consider the transient changes caused by natural convection and the effect of temperature on dielectric properties. Only the electromagnetic phenomena following the approach of Zhang and Datta [10] were taken into account. The electromagnetic field distribution in the oven cavity was calculated using waveform of electric field (Equation 2) obtained from Maxwell's equations [14].

$$\vec{\nabla} \times (\vec{\nabla} \times \vec{E}) - (2\pi f)^2 \varepsilon_0 \mu_0 \varepsilon_c \vec{E} = 0 \quad (2)$$

where $\vec{E}$ is the electric field vector, f is the microwaves frequency, μ_0 is the permeability of free space, ε_0 is the permittivity of free space, ε_c is the complex relative permittivity ($\varepsilon_c = \varepsilon' - j\varepsilon''$), with ε' as the dielectric constant and ε'' as the loss factor), and $\vec{\nabla}$ is the gradient operator.

The metallic cavity and waveguide walls can be approached as perfect electric conductors, to which the following boundary condition applies:

$$\vec{n} \times \vec{E} = 0 \tag{3}$$

where $\vec{n}$ is the unit normal vector.

The tangential component of the electric field is continuous at the interface between two materials air-glass, air-water, and water-glass:

$$\vec{n} \times \left(\vec{E}_1 - \vec{E}_2\right) = 0 \tag{4}$$

where, $\vec{E}_1$ and $\vec{E}_2$ are the electric field in materials 1 and 2, respectively.

The excitation of the microwave oven was modeled through a rectangular waveguide at TE10 mode. In this transverse electric mode, the electric field is perpendicular to the wave direction propagation and shows the half-sine wave distribution, as represented by Equation (5).

$$\vec{E} = \begin{cases} 0 \\ E_0 \sin\left(\dfrac{\pi x^*}{a}\right) \\ 0 \end{cases} \tag{5}$$

where E_0 is the electric field strength at the port; a is the longest side of the rectangular waveguide and x^* is the position relative to dimension a, originating at a/2. The power transmitted at the excitation port (P_{in}) can be correlated to the electric field strength (E_0 calculated with equation 8 from experimental data) by Equation (6).

$$P_{in} = \frac{{E_0}^2 ab}{4\eta_{TE}} \tag{6}$$

where a and b are the cross-section dimensions of the waveguide, with a > b; and η_{TE} is the intrinsic impedance of the wave in the electric transverse mode [14].

The interaction of microwaves with the water converts electromagnetic radiation into thermal energy. The local energy dissipated in the fluid was estimated by the Poynting's theorem (Equation 7), and the total power dissipated (P_{cal}) was calculated through the volume integration of the Equation 7 [6].

$$Q_{MW}(x, y, z) = 2\pi\varepsilon_0\varepsilon'' f\left|\vec{E}\right|^2 \tag{7}$$

Input parameters for the model

The dielectric properties and values of wave-length microwaves (λ) inside each material are summarized in Table 2. The attenuation constant (α) and the microwave power penetration ($d_p = 1/2\alpha$ [27]) in the water were 23.56 m^{-1} and 21.22 mm, respectively.

Table 2. Dielectric properties of air, water, polypropylene, and borosilicate glass.

Material	Dielectric properties			Source
	ε'	ε''	λ (cm)[1]	
Air	1.00	0.0	12.245	Assumed
Water (30 °C)	75.70	8.0	1.405	[20]
Polypropylene	2.40	0.0	7.904	[21]
Borosilicate glass	4.05	0.0	6.085	[22]

[1]calculated.

The electric field strength at the excitation port (E_0) was estimated according to the Zhang and Datta [10] approach. The procedure consists of comparing the power absorbed by a water load (2 kg) in the microwave

oven, determined experimentally (P_{exp}, Equation 1), with the power calculated by the electromagnetic model (P_{cal}) using an arbitrary E_0' value. The E_0 at the excitation port is then estimated using Equation 8.

$$E_0 = E_0' \sqrt{\frac{P_{exp}}{P_{cal}'}} \tag{8}$$

Numerical solution

The mathematical model was solved using the commercially available finite element software COMSOL Multiphysics® 6.0. The waveform equation of the electric field was solved by the RF Module using the interface Frequency Domain and the GMRES iterative solver (Generalized Minimal Residual Method) with the Geometric Multigrid preconditioner and tolerance of 10^{-3}.

Tetrahedral mesh elements with second-order interpolation function were used for discretization of the computational domain. A study on mesh independence was carried out to define the most appropriate mesh size for this model. The normalized power absorption (NPA) was used as a mesh size criterion [8,31].

$$NPA = \frac{P_{cal}}{P_{in}} \tag{9}$$

Figure 2 (a) shows that the NPA values change as the number of elements is increased until converging to a value independent from the number of elements. The NPA results were used to define the element sizes for generating the mesh: 1.5 cm for air domain, and 3 mm for water load. Figure 2 (b) illustrates the differences in mesh size elements of the numerical mesh for the solution of the model. The simulations were performed on an Intel i9-9900x @ 3.5 GHz workstation with 128 GB RAM.

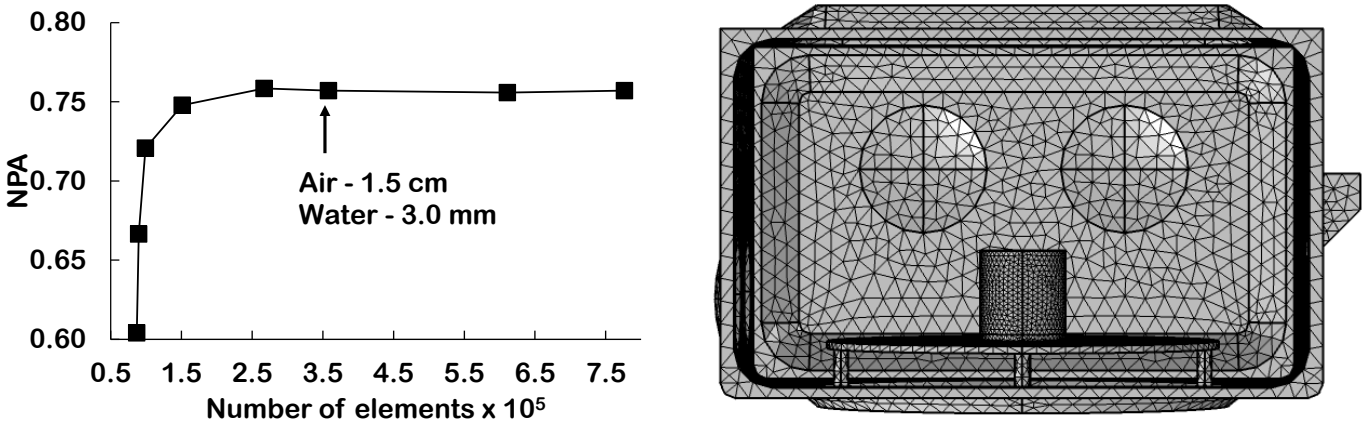

Figure 2. (a) Numerical mesh independence study of mathematical model; (b) Numerical mesh for solution of the model (0.15 kg water load).

Statistical parameters

The absorbed power distribution uniformity was evaluated by the coefficient of variation (COV), which is the ratio between microwave power density standard deviation (SD_{QW}) and mean value ($\overline{Q}_{MW}$). A lower coefficient of variation means a better absorbed microwave power uniformity in the water loads [12,15].

$$COV = \frac{SD_{QW}}{\overline{Q}_{MW}} \tag{10}$$

$$\overline{Q}_{MW} = \frac{\sum_{i=1}^{n} Q_{MW,i}}{n} \tag{11}$$

$$SD_{QW} = \sqrt{\frac{\sum_{i=1}^{n} \left(Q_{MW,i} - \overline{Q}_{MW}\right)^2}{n}} \tag{12}$$

Where **i** represents the *ith* mesh element and **n** is the total number of elements in the mesh.

RESULTS AND DISCUSSION

Model validation

The actual power delivered by the microwave oven (P_{in}, Equation 6, was calculated from electric field strength at the excitation port (E_0) obtained experimentally by Equation 8) was 696.2 W, which was around 70% of the rated power of the oven (1000 W). This result is consistent with those of Soltysiak and coauthors [23], who found values between 90% and 74% of rated power for different household ovens.

Figure 3 shows the power dissipated in water loads obtained experimentally (P_{exp}) and predicted from the mathematical model (P_{cal}). The dissipated power is sensitive to water load size, presenting values that ranged from 700 W (1.5 kg) to 560 W (0.15 kg), but there was no direct correlation between P and m_w. The model shows a good predictive capacity: the relative error was 7.7% in the worst case (1.5 kg water load), and the average error was around 5.2%, considering all cases.

Yi and coauthors [32] showed that a computational domain with detailed cavity design features, such as magnetron, waveguide, and cavity depressions, improves the predictions of electromagnetic models. They found that dents on cavity walls greatly affect the microwave power dissipated in the sample. The detailed description of the computational domain used in the present model can explain the accuracy of the predictions.

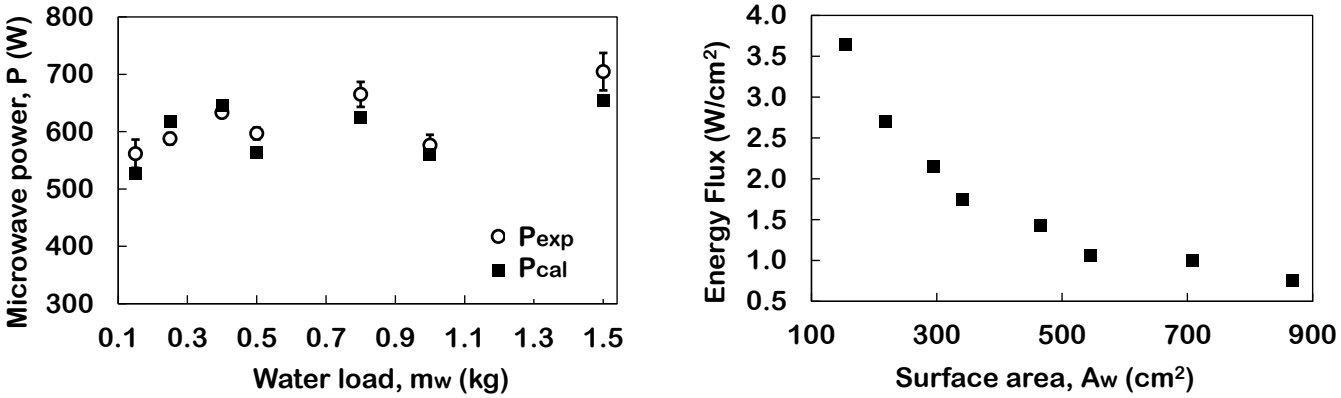

Figure 3. (a) Effect of load size on total microwave power absorption in water. Numerical predictions (P_{cal}) and experimental values (P_{exp}); (b) Surface energy flux (P_{exp}/A_w) as a function of water surface area (A_w).

The surface energy flux is defined as the total power absorbed by the water load divided by the total surface area of the water load; the surface energy flux based on the experimental data is shown in Figure 3b. The energy flux decreases as the surface area increases. Zhang and Datta [10] found a similar trend of surface flux for cylindrical water containers. This trend is attributed to small variations in power absorption when compared to increases in volume and surface area.

Electric field and microwave power density

Figure 4 presents the electric field distribution in the oven cavity with water loads of 1.50, 0.80, and 0.25 kg. Regions of high and low electric fields are obtained into the cavity alternately. Such electric field patterns are characteristic of microwave cavities and lead to a non-uniform heating profile in the water loads (Figure 4) [4,33–35]. Changing the load size changes the resonant-modes of the electromagnetic waves inside the cavity and, consequently, the microwave power dissipated in the sample, as also shown in Figures 4 and 5, respectively.

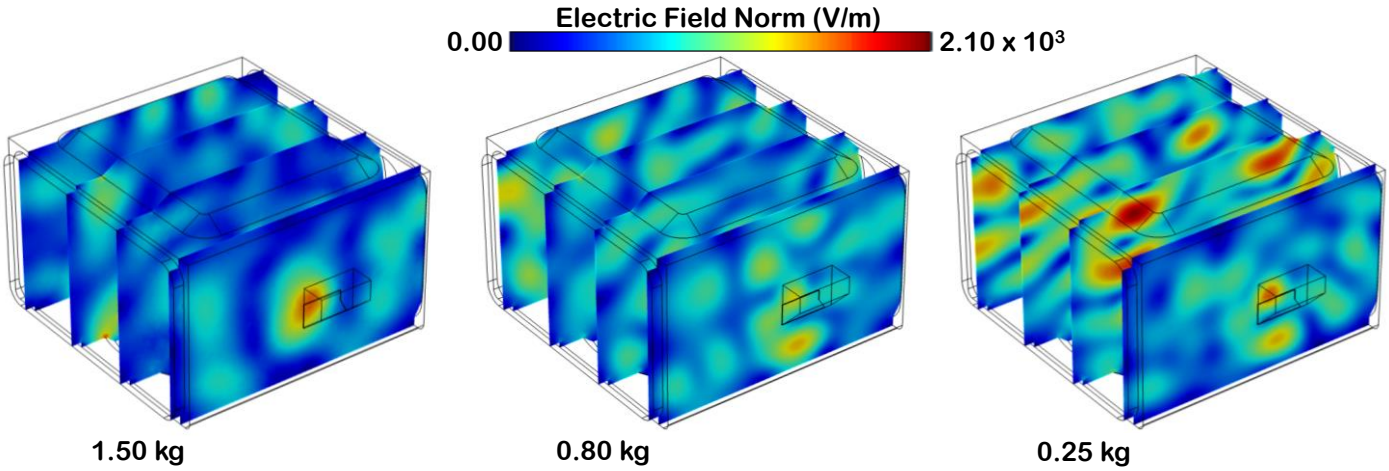

Figure 4. Electric field distribution, E (V/m), in oven cavities with 1.50, 0.80, and 0.25 kg water load.

The profiles of dissipated power (Q_{MW}, Equation 7) in the water loads showed in Figure 5 are the result of resonances that occur when electromagnetic waves penetrate through the sample and a part of the wave reflects from the other end. Transmission and reflection lead to the formation of a series of transmitted and reflected waves and to subsequent constructive/destructive interferences between the waves, resulting in a non-uniform power dissipation [11,36–38].

An energy concentration at the center of the water samples (focusing) was observed, especially for load size below 0.5 kg. When the plane wave is radially incident on the cylinder, the wave transmitted to the water is refracted to the center of the sample, following the well-known Snell's law [37,38]. This overheating effect in the center occurs for diameters of approximately one to three times the penetration depth in water (inner diameter ≈ 1 - 3 d_p) [39]. The heating was mostly near the surface (not focusing) for large samples, as shown in Figure 5, for the load size of 2 kg and 1.5 kg. According to Ayappa and coauthors [40], the intensity of resonances decreases as the sample size increases due to attenuation within the sample, which is consistent with the results found here. Similar dynamics was also found by Su and coauthors [41] during heating of cylindric samples of different sizes in a microwave cavity.

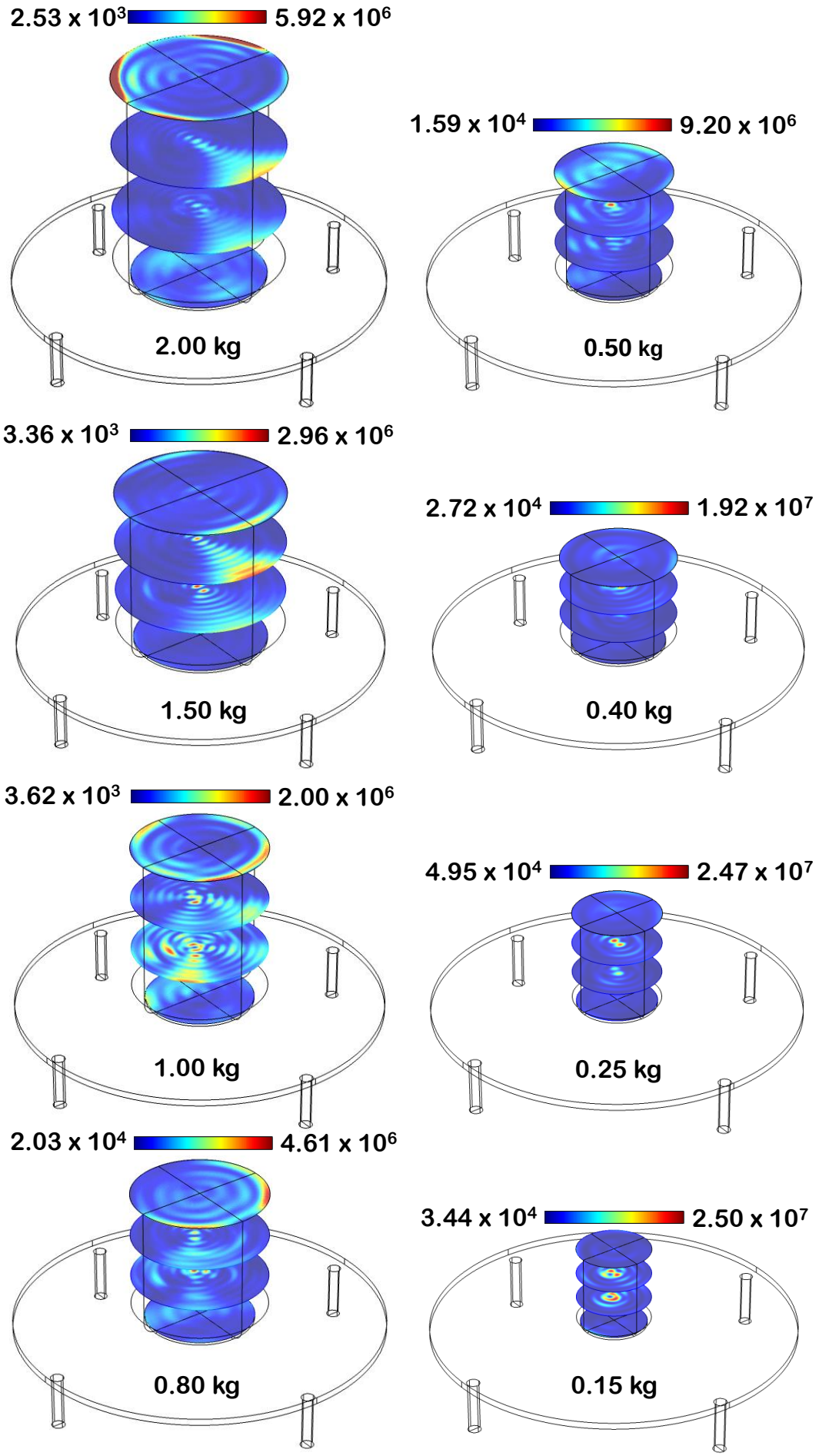

Figure 5. Microwave power density, Q_{MW} (W/m³) (Equation 7), in different load size.

The coefficient of variation (COV) is an indicator of the effective distribution of microwave power. Figure 6 shows that the COV values decrease as the load size was increased from 0.15 kg to 0.5 kg. However, the COV increases when the mass increases beyond 0.5 kg. A low COV value indicates that the relative standard deviation is small for a certain mean value, which is desirable for heating uniformity [15]. The highest COV values were observed for the water mass 2 kg and 1.5 kg. In these conditions, the power dissipation occurs near the surface (Figure 5), i.e., when the effects of microwaves resonance inside the samples are low.

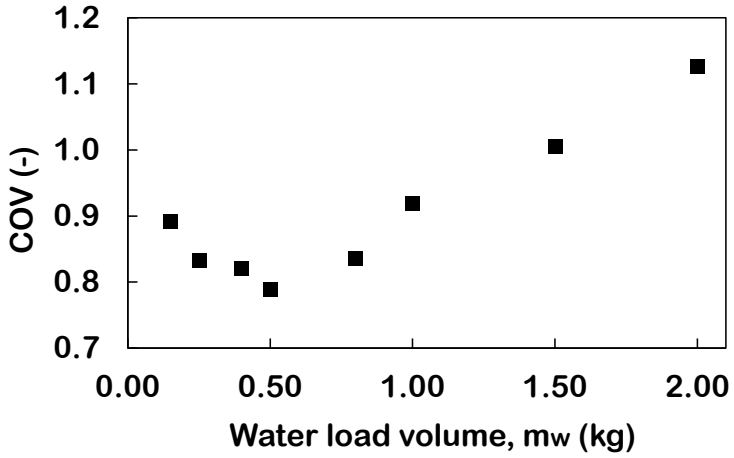

Figure 6. Coefficient of variation (COV) of microwave power density as a function of load size.

Parametric study

A parametric study was performed to quantify the effect of geometrical dimensions of cylindrical samples on the power absorbed by the water load. Table 3 shows 7 sample groups (m_w = 5, 2, 1, 0.5, 0.25, 0.15, and 0.075 kg, assuming water density as constant, ρ_W = 1000 kg m^{-3} = 1kg dm^{-3}), with increasing radius (r) and decreasing height (h). These samples were placed in the middle of the polypropylene table for numerical analysis and the simulations were performed for a constant input power density (P_{in}/m_w), defined as the power delivered by the magnetron (P_{in}) divided by the water mass (m_w).

Table 3. Characteristic dimensions (*r*=radius and *h*=height) of cylindric water loads.

m_w (kg)	5.000	2.000	1.000	0.500	0.250	0.150	0.075
***r* (mm)**	***h* (mm)**						
12.5							152.8
25.0					127.3	76.3	38.2
50.0			127.3	63.7	31.8	19.1	
75.0		113.2	56.6	28.3	14.1		
100.0	151.9	63.7	31.8	15.9			
125.0	101.8	40.7	20.4				
150.0	70.7	28.3	14.1				

The normalized power absorption ($NPA = P_{cal}/P_{in}$) of a water volume is different in different geometrical dimensions of the cylindric samples (Figure 7a). Considering the range of values used here (Table 3), a complex relationship between power density (P_{cal}/m_w) and ratio of the dimensions (2r/h) was found, as shown in Figure 7b. Houšová and Hoke [13] compared the experimental power absorbed in 250 mL of water heated in four glass beakers of different dimensions and found no simple dependence between geometrical dimensions and microwave energy. Zhang and coauthors [12] simulated microwave heating of potato cylinders with constant volume and observed fluctuation in absorbed power as the radius was increased and the height was decreased, as also observed in the present study. Changes in the relationship between sample radius and height led to modification of the electromagnetic wave resonant modes inside the oven cavity, which can explain the complex dynamics observed in Figures 7a, 7b.

The relationship between COV and water load (different dimensions) is shown in Figure 7c. A trend of increasing COV with mass was revealed (similar dynamics as that shown in Figure 6), which is consistent with the findings of Zhangand coauthors [12] and Su and coauthors [41]. However, no correlation was found between COV and ratio of geometrical dimensions of the sample (2r/h) (data not shown).

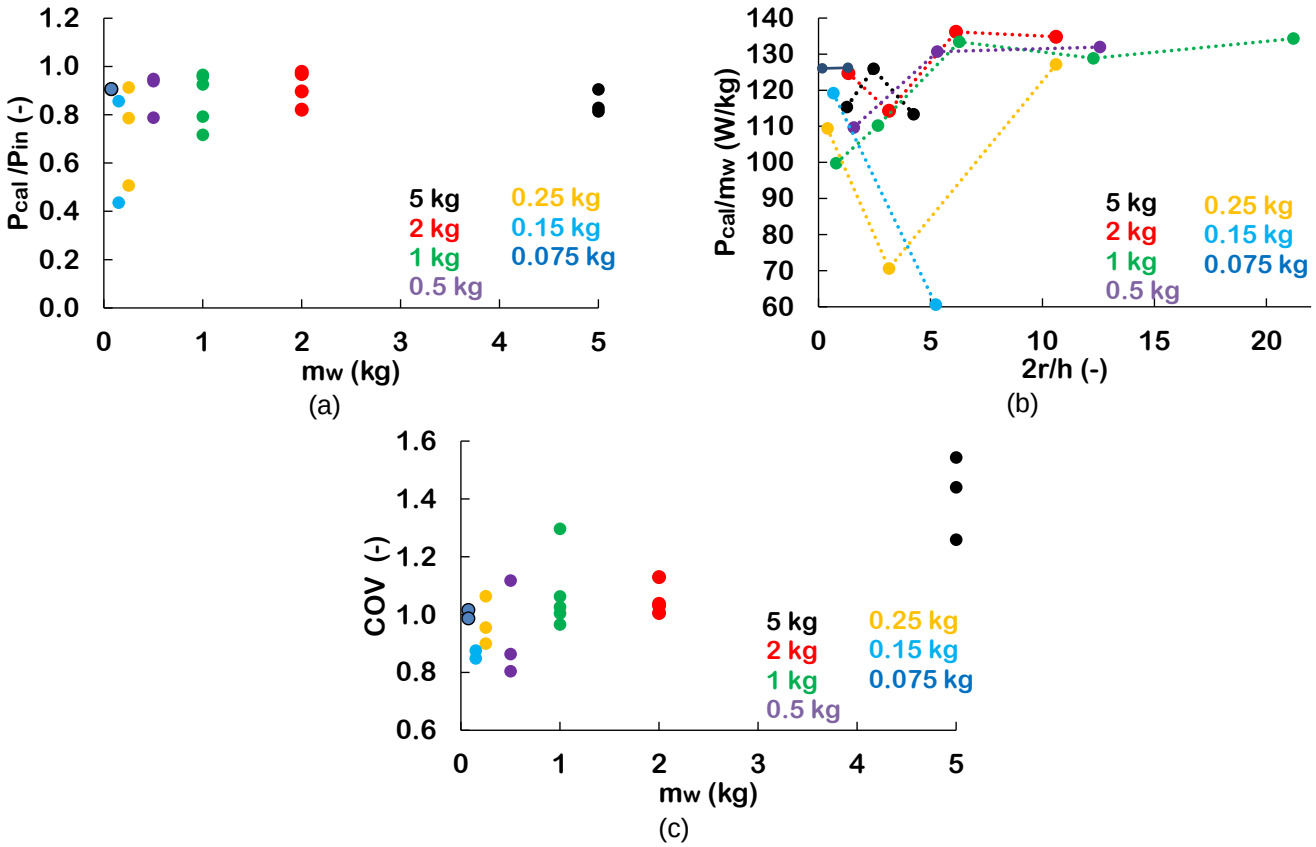

Figure 7. Effect of mass (a) and aspect ratio (b) on power absorption in water. Effect of mass (c) on COV of microwave power density.

CONCLUSION

Maxwell's equations of electromagnetism were solved for a domestic microwave oven to evaluate the power dissipated in water samples. The model described the experimental data accurately and showed the complex dynamics of the electric fields inside the cavity and water (cylindrical shape). Based on numerical results, the distribution of the microwave power density in the water changed with changes in the sample size. The heating uniformity was lower for greater water masses. Furthermore, the amounts of absorbed power also differed for equal mass samples with different characteristic dimensions: radius and height. The modification of the resonance mode of electromagnetic waves inside the oven may explain the dynamics observed. These results indicate that the heating patterns of the microwave oven are the result of combined characteristics of shape and size, as well as the oven cavity.

Conflicts of Interest: It is declared that there is no conflict of interest in publication of this study.

REFERENCES

1. Taşkıran M, Olum E, Candoğan K. Changes in chicken meat proteins during microwave and electric oven cooking. J Food Process Preserv [Internet]. 2020 Feb 17;44(2). Available from: https://onlinelibrary.wiley.com/doi/10.1111/jfpp.14324
2. Teleken JT, Quadri MB, Oliveira APN, Laurindo JB, Datta AK, Carciofi BAM. Mechanistic understanding of microwave-vacuum drying of non-deformable porous media. Dry Technol [Internet]. 2020 Feb 19;1–18. Available from: https://www.tandfonline.com/doi/full/10.1080/07373937.2020.1728303
3. Teleken J, Porciúncula BDA, Teleken JG, Carciofi BAM. Drying of foods under intermittent supply of microwave energy: proposal for a mathematical model. Acta Sci Technol [Internet]. 2021 Jun 14;43:e51037. Available from: https://periodicos.uem.br/ojs/index.php/ActaSciTechnol/article/view/51037
4. Pitchai K, Chen J, Birla S, Jones D, Gonzalez R, Subbiah J. Multiphysics modeling of microwave heating of a frozen heterogeneous meal rotating on a turntable. J Food Sci [Internet]. 2015;80(12):E2803--E2814. Available from: http://doi.wiley.com/10.1111/1750-3841.13136
5. Tang J, Hong Y-K, Inanoglu S, Liu F. Microwave pasteurization for ready-to-eat meals. Curr Opin Food Sci [Internet]. 2018 Oct;23:133–41. Available from: https://linkinghub.elsevier.com/retrieve/pii/S2214799318300201
6. Datta AK, Anatheswaran RC. Handbook of microwave technology for food applications. New York: Marcel Dekker; 2001.

7. Gao X, Liu X, Yan P, Li X, Li H. Numerical analysis and optimization of the microwave inductive heating performance of water film. Int J Heat Mass Transf [Internet]. 2019 Aug;139:17–30. Available from: https://linkinghub.elsevier.com/retrieve/pii/S0017931019301978
8. Zhu J, Kuznetsov AV, Sandeep KP. Mathematical modeling of continuous flow microwave heating of liquids (effects of dielectric properties and design parameters). Int J Therm Sci [Internet]. 2007 Apr;46(4):328–41. Available from: https://linkinghub.elsevier.com/retrieve/pii/S1290072906001153
9. Resurreccion FP, Luan D, Tang J, Liu F, Tang Z, Pedrow PD, et al. Effect of changes in microwave frequency on heating patterns of foods in a microwave assisted thermal sterilization system. J Food Eng [Internet]. 2015 Apr;150:99–105. Available from: https://linkinghub.elsevier.com/retrieve/pii/S0260877414004208
10. Zhang H, Datta AK. Microwave power absorption in single - and multiple - item foods. Food Bioprod Process [Internet]. 2003;81(3):257–65. Available from: https://linkinghub.elsevier.com/retrieve/pii/S0960308503703800
11. Bhattacharya M, Basak T. A comprehensive analysis on the effect of shape on the microwave heating dynamics of food materials. Innov Food Sci Emerg Technol [Internet]. 2017 Feb;39:247–66. Available from: https://linkinghub.elsevier.com/retrieve/pii/S146685641630769X
12. Zhang Z, Su T, Zhang S. Shape Effect on the Temperature Field during Microwave Heating Process. J Food Qual [Internet]. 2018;2018:1–24. Available from: https://www.hindawi.com/journals/jfq/2018/9169875/
13. Houšová J, Hoke K. Microwave heating – the influence of oven and load parameters on the power absorbed in the heated load. Czech J Food Sci [Internet]. 2011 Nov 18;20(No. 3):117–24. Available from: http://www.agriculturejournals.cz/web/cjfs.htm?volume=20&firstPage=117&type=publishedArticle
14. Sadiku MNO. Elements of electromagnetics. 5th ed. Porto Alegre: Bookman, Inc.; 2012.
15. Salvador A, Teleken J, Travassos XL, Avila SL, Carciofi B. Multiphysics Modeling to Assist Microwave Cavity Design for Food Processing. Int J Electr Comput Eng Res [Internet]. 2022 Jun 15;2(2):1–10. Available from: https://www.ijecer.org/ijecer/article/view/233
16. Zhang Y, Yang H, Yan B, Zhu H, Gao W, Zhao J, et al. Continuous flow microwave system with helical tubes for liquid food heating. J Food Eng [Internet]. 2021 Apr;294:110409. Available from: https://linkinghub.elsevier.com/retrieve/pii/S0260877420304957
17. Gulati T, Zhu H, Datta AK, Huang K. Microwave drying of spheres: Coupled electromagnetics-multiphase transport modeling with experimentation. Part II: Model validation and simulation results. Food Bioprod Process [Internet]. 2015;96:326–37. Available from: https://linkinghub.elsevier.com/retrieve/pii/S0960308515001030
18. Datta A, Nicolaï B, Vitrac O, Verboven P, Erdogdu F, Marra F, et al. Computer-aided food engineering. Nat Food [Internet]. 2022 Nov 3;3(11):894–904. Available from: https://www.nature.com/articles/s43016-022-00617-5
19. Chen F, Warning AD, Datta AK, Chen X. Susceptors in microwave cavity heating: Modeling and experimentation with a frozen pie. J Food Eng [Internet]. 2017 Feb;195:191–205. Available from: https://linkinghub.elsevier.com/retrieve/pii/S0260877416303417
20. Jung H, Lee MG, Yoon WB. Effects of Container Design on the Temperature and Moisture Content Distribution in Pork Patties during Microwave Heating: Experiment and Numerical Simulation. Processes [Internet]. 2022 Nov 13;10(11):2382. Available from: https://www.mdpi.com/2227-9717/10/11/2382
21. da Costa FO, Alvarenga TF, de Mesquita TVC, Petri Júnior I. Hybrid drying of pulped arabica coffee cherry beans (Coffea arabica L. cv. Catuai) using a hexagonal microwave dryer designed by numerical simulations. J Food Process Eng [Internet]. 2021 May 23;44(5). Available from: https://onlinelibrary.wiley.com/doi/10.1111/jfpe.13666
22. Llave Y, Kambayashi D, Fukuoka M, Sakai N. Power absorption analysis of two-component materials during microwave thawing and heating: Experimental and computer simulation. Innov Food Sci Emerg Technol [Internet]. 2020 Dec;66:102479. Available from: https://linkinghub.elsevier.com/retrieve/pii/S1466856420304252
23. Soltysiak M, Erle U, Malgorzata C. Load curve estimation for microwave ovens: Experiments and electromagnetic modelling. In: MIKON 2008 – 17th International Conference on Microwaves, Radar and Wireless Communications. Wroclaw, Poland: IEEE; 2008.
24. Monteiro RL, Carciofi BAM, Marsaioli A, Laurindo JB. How to make a microwave vacuum dryer with turntable. J Food Eng [Internet]. 2015;166:276–84. Available from: https://linkinghub.elsevier.com/retrieve/pii/S0260877415002848
25. Bergman TL, Lavine AS, Incropera FP, DeWitt DP. Fundamentals of heat and mass transfer. 7th ed. NY: John Wiley & Sons; 2011.
26. Vries T De. Specific Heat of Pyrex Glass from 25° to 175° C. 1. Ind Eng Chem [Internet]. 1930 Jun 1;22(6):617–8. Available from: https://pubs.acs.org/doi/abs/10.1021/ie50246a017
27. Tang J. Unlocking Potentials of Microwaves for Food Safety and Quality. J Food Sci [Internet]. 2015 Aug 4;80(8). Available from: https://ift.onlinelibrary.wiley.com/doi/10.1111/1750-3841.12959
28. Gezahegn YA, Tang J, Sablani SS, Pedrow PD, Hong Y-K, Lin H, et al. Dielectric properties of water relevant to microwave assisted thermal pasteurization and sterilization of packaged foods. Innov Food Sci Emerg Technol [Internet]. 2021 Dec;74:102837. Available from: https://linkinghub.elsevier.com/retrieve/pii/S1466856421002381
29. Chaki TK, Khastgir DK. Effect of Frequency and Temperature on Dielectric Properties of Polypropylene at X-Band Microwave Region. J Elastomers Plast [Internet]. 1990 Jan 26;22(1):58–71. Available from: http://journals.sagepub.com/doi/ 10.1177/009524439002200107
30. Meredith R. Engineers' Handbook of Industrial Microwave Heating. London/UK: The Institution of Electrial Engineers; 1998.

31. Geedipalli SSR, Rakesh V, Datta AK. Modeling the heating uniformity contributed by a rotating turntable in microwave ovens. J Food Eng [Internet]. 2007 Oct;82(3):359–68. Available from: https://linkinghub.elsevier.com/retrieve/pii/S0260877407001434
32. Yi Z, Qiu W, Jiao Y, Row KH, Cheng Y, Jin Y. Calculation of electric field and temperature distribution within a microwave oven with realistic geometric features geometric features using numeric simulations. J Microw Power Electromagn Energy [Internet]. 2021 Jan 2;55(1):3–27. Available from: https://www.tandfonline.com/doi/full/10.1080/08327823.2020.1838048
33. Chen J, Pitchai K, Birla S, Negahban M, Jones D, Subbiah J. Heat and mass transport during microwave heating of mashed potato in domestic oven-model development, validation, and sensitivity analysis. J Food Sci [Internet]. 2014;79(10):E1991--E2004. Available from: http://doi.wiley.com/10.1111/1750-3841.12636
34. Rakesh V, Seo Y, Datta AK, McCarthy KL, McCarthy MJ. Heat transfer during microwave combination heating: Computational modeling and MRI experiments. AIChE J [Internet]. 2010;NA--NA. Available from: http://doi.wiley.com/10.1002/aic.12162
35. Shen L, Gao M, Feng S, Ma W, Zhang Y, Liu C, et al. Analysis of heating uniformity considering microwave transmission in stacked bulk of granular materials on a turntable in microwave ovens. J Food Eng [Internet]. 2022 Apr;319:110903. Available from: https://linkinghub.elsevier.com/retrieve/pii/S0260877421004295
36. Ayappa KG, Davis HT, Crapiste G, Davis EA, Gordon J. Microwave heating: an evaluation of power formulations. Chem Eng Sci [Internet]. 1991;46(4):1005–16. Available from: https://linkinghub.elsevier.com/retrieve/pii/000925099185093D
37. Zhang H, Datta AK. Heating concentrations of microwaves in spherical and cylindrical foods: Part one: in planes waves. Food Bioprod Process [Internet]. 2005 Mar;83(1):6–13. Available from: https://linkinghub.elsevier.com/retrieve/pii/S0960308505704582
38. Zhang H, Datta AK. Heating concentrations of microwaves in spherical and cylindrical foods: Part Two: in a Cavity. Food Bioprod Process [Internet]. 2005 Mar;83(1):14–24. Available from: https://linkinghub.elsevier.com/retrieve/pii/S0960308505704594
39. Wäppling Raaholt B. Influence of food geometry and dielectric properties on heating performance. In: Erle U, Pesheck PS, Lorence M, editors. Development of Packaging and Products for Use in Microwave Ovens. 2nd ed. Elsevier, Woodhead Publishing; 2020.
40. Ayappa KG, Davis HT, Barringer SA, Davis EA. Resonant microwave power absorption in slabs and cylinders. AIChE J [Internet]. 1997 Mar;43(3):615–24. Available from: https://onlinelibrary.wiley.com/doi/10.1002/aic.690430307
41. Su T, Zhang W, Zhang Z, Wang X, Zhang S. Energy utilization and heating uniformity of multiple specimens heated in a domestic microwave oven. Food Bioprod Process [Internet]. 2022 Mar;132:35–51. Available from: https://linkinghub.elsevier.com/retrieve/pii/S0960308521001991